

Paramagnetism of Tetranuclear Complexes between TCNX Ligands (TCNE, TCNQ, TCNB) and Four Pentaammineruthenium or Dicarbonyl(pentamethylcyclopentadienyl)manganese Fragments

Eberhard Waldhör and Wolfgang Kaim*

Institut für Anorganische Chemie der Universität, Pfaffenwaldring 55,
D-70550 Stuttgart, Germany

Max Lawson and Jeanne Jordanov*

Centre d'Etudes Nucléaires de Grenoble, DRFMC/SCIB/SCPM, 85 X,
F-38054 Grenoble Cedex 09, France

Received August 14, 1996[⊗]

The tetranuclear complexes $\{(\mu_4\text{-TCNX})[\text{Ru}(\text{NH}_3)_5]_4\}(\text{A})_8$ and $(\mu_4\text{-TCNX})[\text{Mn}(\text{CO})_2(\text{C}_5\text{Me}_5)]_4$ [$\text{A} = \text{PF}_6$ or CF_3SO_3 ; TCNX = TCNE (tetracyanoethene), TCNQ (7,7,8,8-tetracyano-*p*-quinodimethane), or TCNB (1,2,4,5-tetracyanobenzene)] were studied by variable-temperature (2–300 K) SQUID susceptometry. Mono- and dinuclear species $[\text{PhCN}]\text{Ru}(\text{NH}_3)_5(\text{PF}_6)_2$ (PhCN = benzonitrile) and $\{(\mu\text{-L})[\text{Ru}(\text{NH}_3)_5]_2\}(\text{PF}_6)_4$ (L = 1,4-dicyanobenzene (terephthalodinitrile) or pyrazine) were also investigated for comparison and were found to be essentially diamagnetic. Despite the even electron count, both the ruthenium and manganese tetranuclear complexes are paramagnetic, albeit with different spin–spin exchange coupling patterns. The manganese systems are characterized by exchange-coupled $S = 1$ states at the individual metal centers, whereas the magnetic behavior of the tetranuclear ruthenium compounds results from an exchange-coupling interaction between two $S = 1/2$ sites, identified as $\text{Ru}^{\text{III}}/\text{Ru}^{\text{II}}$ mixed-valence pairs.

Introduction

Transition metal compounds of TCNE, TCNQ, and related unsaturated polynitrile ligands¹ have recently played a prominent role in the development of “designer magnets”^{2–4} within the new area of molecular magnetism.^{2–5} The “TCNX” ligands¹ are very unusual because of their variable coordination behavior (σ or π), their established ability to bridge up to four metal centers, their propensity to form aggregates via π/π interaction (stacking), and their “noninnocence”, i.e. their facile reduction to radical anions or dianions.¹ Exhaustive μ_4, η^4 -coordination of TCNE or TCNQ has been reported so far only for discrete ruthenium⁶ and manganese complexes⁷ and for a structurally characterized coordination polymer $\{(\text{TCNE})[\text{Rh}_2(\text{O}_2\text{CCF}_3)_4]_2\}_\infty$.⁸

Among the several remarkable products of the intricate transition metal coordination chemistry of the TCNX ligands is the polymeric material $[\text{V}(\text{TCNE})_x]_n \cdot y \text{CH}_2\text{Cl}_2$ ($x \approx 2$, $y \approx 0.5$) from the reaction between $\text{V}(\text{C}_6\text{H}_6)_2$ and TCNE which exhibits ferrimagnetic behavior up to 350 K ($T_c \approx 400$ K).^{2–4,9} Due to the insolubility of this amorphous material, its charac-

terization is based largely on elemental analysis and vibrational spectroscopy; a first dinuclear organovanadium complex of TCNE was identified recently as a $\text{V}^{\text{IV}}(\mu\text{-TCNE}^{2-})\text{V}^{\text{IV}}$ species.¹⁰ Other magnetic compounds with TCNX ligands include a (porphinato)manganese(III) complex of $\mu\text{-TCNE}$ (ferrimagnet, $T_c = 14$ K),¹¹ decamethylferrocene/TCNE (ferromagnet, $T_c = 4.8$ K),¹² and decamethylferrocene/TCNQ (ferromagnet, $T_c = 2.55$ K).^{13,14}

While exploring the electron transfer and oligonucleation behavior of TCNX ligands, we discovered the unexpected paramagnetism of complexes $(\mu_n, \eta^u\text{-L})[\text{Mn}(\text{CO})_2(\text{C}_5\text{Me}_5)]_n$ with ligands L such as pyridine ($n = 1$), pyrazine ($n = 2$), or TCNE ($n = 4$).¹⁵ The unusual phenomenon that organometallic 18 valence electron centers display such paramagnetism at ambient temperatures was attributed¹⁵ to the occupation of $S = 1$ magnetically excited states which become accessible because of low symmetry, a weak ligand L, and the well-known small ligand-field splitting of low-valent manganese.

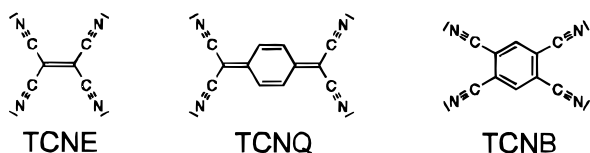
Considering the similarity¹⁶ of the organometallic 16 valence electron fragments $\text{Mn}(\text{CO})_2(\text{C}_5\text{R}_5)$ with $[\text{Ru}(\text{NH}_3)_5]^{2+}$

[⊗] Abstract published in *Advance ACS Abstracts*, June 15, 1997.

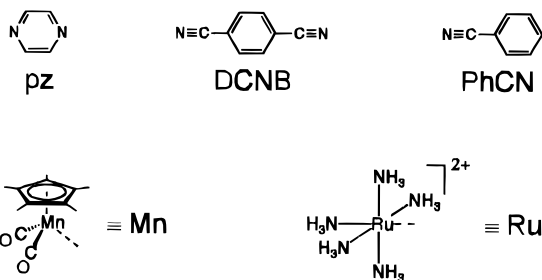
- (1) Kaim, W.; Moscherosch, M. *Coord. Chem. Rev.* **1994**, *129*, 157.
- (2) Miller, J. S.; Epstein, A. J. *Angew. Chem.* **1994**, *106*, 399; *Angew. Chem., Int. Ed. Engl.* **1994**, *33*, 385.
- (3) (a) Miller, J. S.; Epstein, A. J. *Chem. Br.* **1994**, 477. (b) Miller, J. S. *Adv. Mater.* **1994**, *6*, 322.
- (4) (a) Miller, J. S.; Epstein, A. J. *Chem. Eng. News* **1995**, Oct 2, 30. (b) Miller, J. S.; Epstein, A. J. *Chem. Ind. (London)* **1996**, 49.
- (5) Kahn, O. *Molecular Magnetism*; VCH: Weinheim, Germany, 1993.
- (6) (a) Moscherosch, M.; Waldhör, E.; Binder, H.; Kaim, W.; Fiedler, J. *Inorg. Chem.* **1995**, *34*, 4326. (b) Moscherosch, M.; Kaim, W. *Inorg. Chim. Acta* **1993**, *206*, 229.
- (7) Gross-Lannert, R.; Kaim, W.; Olbrich-Deussner, B. *Inorg. Chem.* **1990**, *29*, 5046.
- (8) Cotton, F. A.; Kim, Y. *J. Am. Chem. Soc.* **1993**, *115*, 8511.
- (9) Manriquez, J. M.; Yee, G. T.; McLean, R. S.; Epstein, A. J.; Miller, J. S. *Science* **1991**, *252*, 1415.

- (10) Baumann, F.; Heilmann, M.; Matheis, W.; Schulz, A.; Kaim, W.; Jordanov, J. *Inorg. Chim. Acta* **1996**, *251*, 239.
- (11) Miller, J. S.; Calabrese, J. C.; McLean, R. S.; Epstein, A. J. *Adv. Mater.* **1992**, *4*, 498.
- (12) Miller, J. S.; Calabrese, J. C.; Rommelmann, H.; Chittipeddi, S. R.; Zhang, J. H.; Reiff, W. M.; Epstein, J. A. *J. Am. Chem. Soc.* **1987**, *109*, 769.
- (13) Miller, J. S.; Reis, A. H., Jr.; Gebert, E.; Ritsko, J. J.; Salaneck, W. R.; Kovnat, L.; Cape, T. W.; Van Duyne, R. P. *J. Am. Chem. Soc.* **1979**, *101*, 7111.
- (14) Broderick, W. E.; Eichhorn, D. M.; Liu, X.; Toscano, P. J.; Owens, S. M.; Hoffman, B. M. *J. Am. Chem. Soc.* **1995**, *117*, 3641.
- (15) Kaim, W.; Roth, T.; Olbrich-Deussner, B.; Gross-Lannert, R.; Jordanov, J.; Roth, E. K. H. *J. Am. Chem. Soc.* **1992**, *114*, 5693.
- (16) Gross, R.; Kaim, W. *Inorg. Chem.* **1986**, *25*, 498.

species,¹⁷⁻¹⁹ we recently⁶ reported the synthesis and electronic structures of complex ions $\{(\mu_4\text{-TCNX})[\text{Ru}(\text{NH}_3)_5]_4\}^{8+}$, TCNX = TCNE, TCNQ, and TCNB (1,2,4,5-tetracyanobenzene), correcting a former report²⁰ on the TCNE derivative. The pentaammineruthenium fragment has played a prominent role in the development of an understanding of thermal and photoinduced electron transfer reactivity.^{17,18,21} It is distinguished by unusually inert bonds between metal and nitrogen donor ligands in both the di- and trivalent states of the metal, by reversible redox processes for the Ru^{II}/Ru^{III} pair at convenient potentials and with small reorganization energies, and by the hydrophilic nature of the resulting complexes.²¹ Furthermore, the 4d⁶ or 4d⁵ ruthenium species are generally assumed to have well-defined electronic structures with low-spin configurations and charge-transfer excited states typically lying lower than ligand-field excited configurations.^{17,18,21}



In this work we report detailed magnetic studies from variable SQUID susceptometry of the compounds $(\mu_4\text{-TCNX})\text{-}[\text{Mn}(\text{CO})_2(\text{C}_5\text{Me}_5)_4]$ (TCNX = TCNE or TCNQ) and $\{(\mu_4\text{-TCNX})[\text{Ru}(\text{NH}_3)_5]_4\}(\text{A})_8$ (A = PF₆ or CF₃SO₃; TCNX = TCNE, TCNQ, or TCNB). The study of the ruthenium compounds was prompted by the observation of broadened ¹H-NMR features in the cases of the TCNE and TCNB complexes.⁶ Mono- and dinuclear species $\{(\mu\text{-L})[\text{Ru}(\text{NH}_3)_5]_2\}(\text{PF}_6)_4$, L = 1,4-dicyanobenzene (terephthalodinitrile)²² or pyrazine,^{18a} and $[(\text{PhCN})\text{Ru}(\text{NH}_3)_5](\text{PF}_6)_2$, PhCN = benzonitrile,²³ were also investigated for comparison. The compounds are represented as follows: $(\mu_4\text{-TCNE})[\text{Mn}(\text{CO})_2(\text{C}_5\text{Me}_5)_4] = [\text{Mn}_4\text{TCNE}]$; $(\mu_4\text{-TCNQ})[\text{Mn}(\text{CO})_2(\text{C}_5\text{Me}_5)_4] = [\text{Mn}_4\text{TCNQ}]$; $\{(\mu_4\text{-TCNE})[\text{Ru}(\text{NH}_3)_5]_4\}(\text{PF}_6)_8 = [\text{Ru}_4\text{TCNE}]$; $\{(\mu_4\text{-TCNQ})[\text{Ru}(\text{NH}_3)_5]_4\}(\text{PF}_6)_8 = [\text{Ru}_4\text{TCNQ}]$; $\{(\mu_4\text{-TCNB})[\text{Ru}(\text{NH}_3)_5]_4\}(\text{CF}_3\text{SO}_3)_8 = [\text{Ru}_4\text{TCNB}]$; $\{(\mu_2\text{-DCNB})[\text{Ru}(\text{NH}_3)_5]_2\}(\text{PF}_6)_4 = [\text{Ru}_2\text{DCNB}]$ (DCNB = 1,4-dicyanobenzene); $\{(\mu_2\text{-pz})[\text{Ru}(\text{NH}_3)_5]_2\}(\text{PF}_6)_4 = [\text{Ru}_2\text{pz}]$ (pz = pyrazine); $\{(\text{PhCN})[\text{Ru}(\text{NH}_3)_5]\}(\text{PF}_6)_2 = [\text{RuPhCN}]$ (PhCN = benzonitrile).



The question of magnetic behavior is related to that of the proper oxidation state formulation with respect to the bridging ligand (TCNX^{0/-2-}) and the four metal centers (Ru^{II/III} or Mn^{II/III}). Results from NMR, IR, UV/vis, and XPS spectroscopy

have indicated highly symmetric arrangements with four equivalent metal sites ML_n in each of the complexes $(\mu_4, \eta^4\text{-TCNX})[\text{ML}_n]_4$, ML_n = Mn(CO)₂(C₅Me₅) or [Ru(NH₃)₅]²⁺, including extensive π conjugation between the TCNX π systems and the metal d _{π} orbitals.^{6,7} However, the assignment of fractional oxidation states as in the general formula $\{(\text{TCNX}^{\delta-})[\text{Ru}^{\text{II}+\delta/4}(\text{NH}_3)_5]_4\}^{n+}$ with $\delta \approx 1.5$ (TCNE, TCNQ) or $\delta < 1.0$ (TCNB)⁶ does not automatically predetermine the spin state of the complex, which is largely based on the interaction and coupling of individual spins centered at the TCNX ligands or the metals.

Experimental Section

Materials. Syntheses, analytical data, and spectroscopic characterization of the tetranuclear complexes $(\mu_4\text{-TCNX})[\text{Mn}(\text{CO})_2(\text{C}_5\text{Me}_5)_4]$ (TCNX = TCNE or TCNQ)^{7,24} and $\{(\mu_4\text{-TCNX})[\text{Ru}(\text{NH}_3)_5]_4\}(\text{A})_8$ (A = PF₆ or CF₃SO₃; TCNX = TCNE, TCNQ, or TCNB)⁶ were reported previously. Mono- and dinuclear species $\{(\mu\text{-L})[\text{Ru}(\text{NH}_3)_5]_2\}(\text{PF}_6)_4$, L = DCNB²² or pyrazine,^{18a} and $[(\text{PhCN})\text{Ru}(\text{NH}_3)_5](\text{PF}_6)_2$ ²³ were also described before. The purity and identity of the substances was confirmed using elemental analysis, UV/vis, and IR vibrational spectroscopy, and cyclic voltammetry. EPR measurements of the solid materials at 3.5 K and ambient temperature showed the absence of noninteger spin states.

Instrumentation. For susceptibility measurements we used a Quantum Design SQUID magnetometer, equipped with a Quantum Design controller MPS 1822 and a digital bridge 1802, operating at 0.5 T magnetic field strength and variable temperature (2–300 K). Magnetization studies were carried out between 0.1 and 1 T at 6 K to determine the most suitable field (i.e. nonsaturation conditions). Typical samples involved 15–25 mg of the compound; all data are corrected for effects from the sample holder and diamagnetic contributions.

Simulations were performed on an IBM-PC using the programs Microsoft Excel 4.0 and Microsoft Excel Solver. Nonlinear minimization of *R* (eq 1) yielded the values of *g*, *J*, *J'* and *TIP* given below.

$$R = \frac{\sum_i [(\chi_M T)_i^{\text{exp}} - (\chi_M T)_i^{\text{calc}}]^2}{\sum_i [(\chi_M T)_i^{\text{exp}}]^2} \quad (1)$$

Different sets of starting values were used to avoid local minima. Being largely independent of the number of data points and the absolute values, *R* allows a comparison of the quality of fit between compounds with widely differing magnetic susceptibilities.

Results

Figure 1 illustrates the behavior of μ_{eff} vs *T* for all pentaammineruthenium compounds investigated. Figure 2 depicts the $\chi_M T$ vs *T* dependence (and simulation; see below) for the

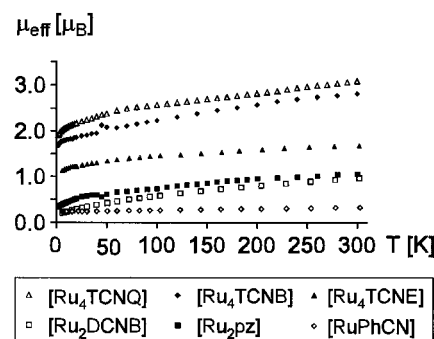


Figure 1. μ_{eff} vs *T* dependence for the pentaammineruthenium complexes.

- (17) Taube, H. *Pure Appl. Chem.* **1975**, *44*, 25.
 (18) (a) Creutz, C.; Taube, H. *J. Am. Chem. Soc.* **1973**, *95*, 1086. (b) Creutz, C. *Prog. Inorg. Chem.* **1983**, *30*, 1.
 (19) Winkler, J. R.; Gray, H. B. *Chem. Rev.* **1992**, *92*, 369.
 (20) Amer, S. I.; Dasgupta, T. P.; Henry, P. M. *Inorg. Chem.* **1983**, *22*, 1970.
 (21) Taube, H. *Angew. Chem.* **1984**, *96*, 315; *Angew. Chem., Int. Ed. Engl.* **1984**, *23*, 329. (b) Taube, H. *Science* **1984**, *226*, 1028.
 (22) Richardson, D. E.; Taube, H. *J. Am. Chem. Soc.* **1983**, *105*, 40.
 (23) Clarke, R. E.; Ford, P. C. *Inorg. Chem.* **1970**, *9*, 227.

- (24) Olbrich-Deussner, B.; Kaim, W.; Gross-Lannert, R. *Inorg. Chem.* **1989**, *28*, 3113.

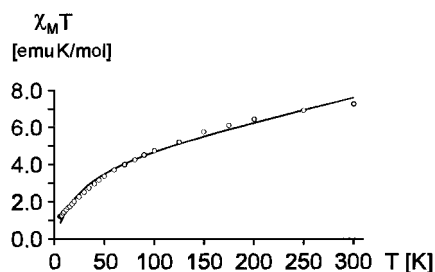


Figure 2. $\chi_M T$ vs T dependence for $(\mu_4, \eta^4\text{-TCNQ})[\text{Mn}(\text{CO})_2(\text{C}_5\text{Me}_5)]_4$ (O). The theoretical curve (full line) was calculated with the data from Table 2.

Table 1. Magnetic Characteristics of Manganese and Ruthenium Complexes at 300 K

compd	$\chi_M T$ (emu K mol ⁻¹)	μ_{eff}
[Mn ₄ TCNQ]	7.257	7.62
[Mn ₄ TCNE]	1.564	3.54
[Ru ₄ TCNQ]	1.181	3.07
[Ru ₄ TCNB]	0.980	2.80
[Ru ₄ TCNE]	0.349	1.67
[Ru ₂ DCNB]	0.144	0.96
[Ru ₂ pz]	0.103	0.91
[RuPhCN]	0.102	0.91

tetranuclear organomanganese complex of TCNQ. Table 1 lists the 300 K values of $\chi_M T$ and μ_{eff} , the latter calculated according to eq 2.

$$\mu_{\text{eff}} = \sqrt{3k\chi_M T/N\beta^2} \approx \sqrt{8\chi_M T} \quad (2)$$

While the mono- and dinuclear ruthenium compounds with the less π accepting ligands benzonitrile, 1,4-dicyanobenzene, and pyrazine exhibit only minute paramagnetism and can be considered essentially diamagnetic, the tetranuclear compounds with the TCNX ligands exhibit sizable paramagnetism, albeit with considerable differences (Figure 1). Whereas the tetranuclear ruthenium–TCNE complex seems to achieve saturation at a μ_{eff} value which would correspond to one unpaired electron in the spin-only formalism, the TCNB and TCNQ complexes reach higher $\chi_M T$ and μ_{eff} values which would correspond to an $S = 1$ (triplet) situation at 300 K but are still far from saturation (Figure 1). In general, the nonlinear $\chi_M T$ vs T behavior suggests a complex magnetic interaction pattern, involving spin–spin exchange phenomena and effects from spin–orbit coupling.

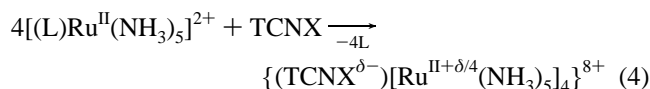
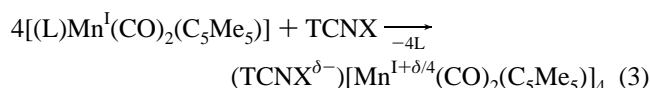
The organomanganese compounds display much larger $\chi_M T$ values and magnetic moments as compared to corresponding pentaammineruthenium complexes (Table 1). Both the lower symmetry (C_s vs C_{4v}) and the 3d instead of 4d transition metal status may be held responsible for this difference. Our previous study¹⁵ has indeed shown that—in contrast to the ruthenium systems reported here—even simple mono- and dinuclear compounds such as (py)Mn(CO)₂(C₅Me₅) or (pz)[Mn(CO)₂(C₅Me₅)₂ are paramagnetic at ambient temperatures, implying an $S = 0$ to $S = 1$ transition for the *individual* manganese centers at rather low temperatures. As for the [Ru₄TCNB] and [Ru₄TCNQ] complexes, there is no saturation at ambient temperatures for the tetranuclear organomanganese compounds.

Discussion

The different magnetic behavior of mono- or dinuclear compounds of Mn(CO)₂(C₅Me₅) and [Ru(NH₃)₅]²⁺ with simple, i.e. redox-innocent, ligands provides a first indication for different spin–spin coupling patterns in the tetranuclear com-

pounds of the TCNX ligands. The sizable paramagnetism of mono- and dinuclear compounds of Mn(CO)₂(C₅Me₅) with weak π acceptor ligands such as pyridine or pyrazine¹⁵ contrasts with the absence of such effects for the related complexes [RuPhCN], [Ru₂DCNB], or [Ru₂pz] (Figure 1). It appears that the magnetically excited states responsible for the remarkable, primarily metal-centered paramagnetism of 18 valence electron organomanganese(I) species are less accessible for otherwise analogous¹⁶ pentaammineruthenium(II) systems. The higher ligand-field symmetry of the latter and the 4d transition metal status probably combine to increase the d orbital splitting sufficiently so as to prevent significant thermal population of magnetically excited states, despite the much lower position of ammonia in the spectrochemical series as compared to carbonyl or $\eta^5\text{-C}_5\text{R}_5$ ligands.

With the noninnocent TCNX ligands the situation is more complex. Although nonreduced tetranitrile ligands TCNX and nonoxidized dicarbonyl(pentamethylcyclopentadienyl)manganese(I) or pentaammineruthenium(II) complex fragments were used in the synthesis of the tetranuclear complexes, it cannot be automatically anticipated that these oxidation states remain unchanged after the 4-fold addition. At least for the highly electron-accepting TCNE and TCNQ systems (the reduction potential of TCNB is more negative by about 0.8 V⁶), a ground-state electron transfer according to eqs 3 and 4 may be considered.



The amount δ of total net metal-to-ligand electron transfer may vary between 0 and 2; δ was estimated from spectroscopic investigations between 1 and 2 for the TCNE and TCNQ compounds and somewhat lower for the TCNB derivative of pentaammineruthenium.^{6,7} An indication for different electronic structures within the ruthenium series came from the observation that the reduction potentials of the complexes with TCNE and TCNQ are more negative than those of the corresponding free ligands whereas the TCNB system displayed the “normal” behavior,²⁴ i.e. a facilitated reduction of the ligand after metal coordination.⁶ For the TCNE and TCNQ complexes one may thus assume that at least one electron equivalent has been transferred from the metals to the TCNX ligand during coordination.^{6,7}

With concern to the overall electronic structure, the frontier MOs of the manganese and ruthenium complexes may be calculated using Hückel MO theory, incorporating all four transition metals as (d) π centers. This approach was successfully employed to interpret the long-wavelength absorption data of the complexes $(\mu_n\text{-TCNE})[\text{Mn}(\text{CO})_2(\text{C}_5\text{Me}_5)]_n$, $n = 1\text{--}4$,⁷ and $\{(\mu_4\text{-TCNX})[\text{Ru}(\text{NH}_3)_5]_4\}^{8+}$, TCNX = TCNE, TCNQ, TCNB, and TCNP (tetracyanopyrazine).⁶

For both the manganese and ruthenium tetranuclear compounds the fitting according to the Curie–Weiss law⁵ produced unsatisfactory results which could be improved using either of two spin–spin exchange coupling models:

(a) Considering *individual* metal centers with $S = 1$ states, the exchange coupling across the TCNX bridging ligand (Scheme 1) can be approximated using the Heisenberg exchange Hamiltonian in eq 5. (b) Intramolecular electron transfer according to eqs 3 or 4 with e.g. $\delta = 2$ can produce a situation

$$\hat{H}_{\text{exc}} = -J_1(\hat{S}_A\hat{S}_B + \hat{S}_C\hat{S}_D) - J_2(\hat{S}_A\hat{S}_C + \hat{S}_B\hat{S}_D) - J_3(\hat{S}_A\hat{S}_D + \hat{S}_B\hat{S}_C) \quad (5)$$

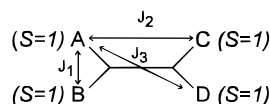
where two strongly coupled mixed-valent sites such as dinitrilo-bridged Ru^{III}/Ru^{II} entities (each with $S_{\text{tot}} = 1/2$) can couple via an essentially diamagnetic (reduced) bridging ligand.^{6b}

Spin-orbit coupling is not directly accounted for in either of these two models (a and b). This could explain remaining incongruities in the simulation of $\chi_{\text{M}}T$ vs T curves (Figures 2 and 3).

We first consider the two tetranuclear organomanganese complexes [Mn₄TCNE] and [Mn₄TCNQ]. The former had been discussed briefly before,¹⁵ while the latter compound with the most pronounced paramagnetism (Table 1, Figure 2) is presented here for the first time. Whereas spin-orbit coupling effects should play a smaller role here than for the ruthenium compounds, the low-symmetry situation at the metal centers can complicate the interpretation.

The large magnetic moments observed for the TCNQ complex and an improved analysis of the paramagnetism¹⁵ of [Mn₄TCNE] could be interpreted using approximation (a) described above, starting from Scheme 1. The magnetic interaction between the four equivalent metal centers A–D with individual $S = 1$ states is described by the Hamiltonian (5).

Scheme 1



The necessary²⁵ approximation to solve the corresponding system of secular equations involves a reduction of variables by setting $J_1 = J$ and $J_2 = J_3 = J'$, since the latter describe interactions mediated by the same number of chemical bonds. The eigenvalue equations provided by the resulting Hamiltonian (6) can be solved by substituting eq 7 to obtain the expression (8) for the energy ladder (Scheme 2).

$$\hat{H}_{\text{exc}} = -J(\hat{S}_A\hat{S}_B + \hat{S}_C\hat{S}_D) - J'(\hat{S}_A\hat{S}_C + \hat{S}_B\hat{S}_D + \hat{S}_A\hat{S}_D + \hat{S}_B\hat{S}_C) \quad (6)$$

$$\hat{S}_{\text{AB}} = \hat{S}_A + \hat{S}_B \quad \hat{S}_{\text{CD}} = \hat{S}_C + \hat{S}_D \quad \hat{S} = \hat{S}_{\text{AB}} + \hat{S}_{\text{CD}} \quad (7)$$

$$E(|S, S_{\text{AB}}, S_{\text{CD}}\rangle) = -\frac{J-J'}{2}[S_{\text{AB}}(S_{\text{AB}}+1) + S_{\text{CD}}(S_{\text{CD}}+1)] - \frac{J'}{2}S(S+1) \quad (8)$$

Inclusion of the axial zero-field splitting parameter D and the Zeeman interaction $g\beta B$ leads to a total of 81 energy eigenvalues (eq 9).

$$E(|S, S_{\text{AB}}, S_{\text{CD}}, S_z\rangle) = -\frac{J-J'}{2}[S_{\text{AB}}(S_{\text{AB}}+1) + S_{\text{CD}}(S_{\text{CD}}+1)] - \frac{J'}{2}S(S+1) + D[S_z^2 - \frac{1}{3}S(S+1)] + g\beta BS_z \quad (9)$$

Combining the coefficients of eq 9 with the VanVleck equation⁵ allowed us to simulate the experimental $\chi_{\text{M}}T$ vs T behavior. Figure 2 shows the result for [Mn₄TCNQ], and Table 2 summarizes the relevant exchange data.

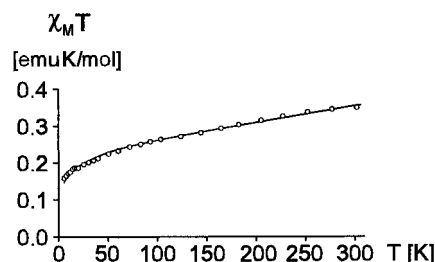
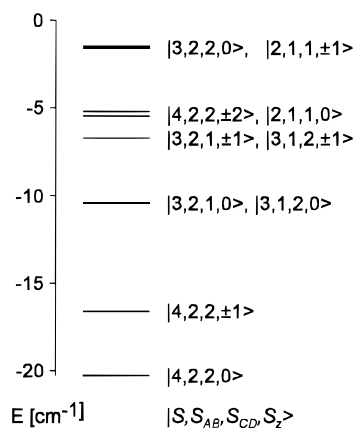


Figure 3. $\chi_{\text{M}}T$ vs T dependence for $\{(\mu_4, \eta^4\text{-TCNE})[\text{Ru}(\text{NH}_3)_5]_4\}(\text{PF}_6)_8$ (O). The theoretical curve (full line) was calculated with the data from Table 2.

Scheme 2



The coupling constants J and J' thus determined suggest that there are small ferromagnetic and antiferromagnetic interactions of comparable absolute magnitude. While J' involves seven intervening chemical bonds but a shorter distance in the cisoid arrangement (see Figure 4), the J interaction runs across only six chemical bonds but involves a larger distance (through-bond vs through-space). Models neglecting one of these interactions could not reproduce the experimental behavior. The values for J , J' , and D of [Mn₄TCNQ] are lower than those calculated for [Mn₄TCNE] (Table 2) which is in agreement with the basic magnetic data (Table 1) and with the expectations for a qualitatively similar but more extended exchange-mediating bridging ligand. The unusually small calculated g factor is paralleled in the ruthenium series (Table 2) and may be due to the nonconsideration of contributions from spin-orbit coupling.

All three tetranuclear pentaammineruthenium complexes exhibit sizable paramagnetism. Paramagnetic ruthenium(II) complexes had been reported for the dinuclear species $\text{Ru}_2(\text{O}_2\text{CR})_4$ where the metal-metal multiple bond formation results in two degenerate π^* orbitals occupied by two electrons.²⁶ The rather small magnetic moment determined for the TCNE derivative [Ru₄TCNE] as compared to that of the TCNQ analogue parallels the observations made in the manganese series. Another similarity concerns the equivalence of all four metal centers^{6,7} and the extensive π conjugation including the metal $d\pi$ orbitals.

However, model a (Scheme 1, eqs 5–9) which was successfully applied to the manganese compounds turned out to be totally unapplicable here, confirming that the observed paramagnetism of the tetra-ruthenium complexes is not a quality of the individual metal centers because of a large ligand-field splitting. Instead, model b involving two exchange-coupled $S = 1/2$ entities, attributed to two mixed-valent Ru^{II}/Ru^{III} sites, allowed us to successfully simulate the experimental $\chi_{\text{M}}T$ vs T curves (Figure 3).

(26) (a) Cotton, F. A.; Ren, T.; Eglin, J. L. *Inorg. Chem.* **1991**, *30*, 2552. (b) Cotton, F. A.; Miskowski, V. M.; Zhong, B. *J. Am. Chem. Soc.* **1989**, *111*, 617.

(25) Belorizky, E.; Fries, P. H. *J. Chim. Phys.* **1993**, *11*, 1077.

Table 2. Magnetic Coupling Data^{a,b} for Tetranuclear Manganese and Ruthenium Complexes with TCNX Ligands

compd	J	J'	D	g	TIP	R^c
[Mn ₄ TCNQ]	-2.2 ± 0.2	2.2 ± 0.2	3.7 ± 0.2	2.05	1.2×10^{-2}	2.0×10^{-3}
[Mn ₄ TCNE]	-3.3 ± 0.2	3.5 ± 0.2	6.0 ± 0.5	1.20	8.9×10^{-4}	3.4×10^{-3}
[Ru ₄ TCNQ]	3.2 ± 0.2		13.7 ± 0.5	1.81	1.9×10^{-4}	3.7×10^{-4}
[Ru ₄ TCNB]	4.0 ± 0.2		9.3 ± 0.5	1.47	2.0×10^{-3}	4.3×10^{-4}
[Ru ₄ TCNE]	8.2 ± 0.5		42.1 ± 1.0	1.10	4.4×10^{-4}	2.6×10^{-4}

^a Determined by simulations of experimental χ_{MT} vs T functions using eq 12 for the ruthenium complexes and formalism (9) for the manganese compounds (see Scheme 1). ^b Exchange coupling constants J and zero-field splitting parameters D in cm^{-1} ; temperature-independent paramagnetism TIP in emu mol^{-1} . ^c For definition of the minimized quantity R , see eq 1.

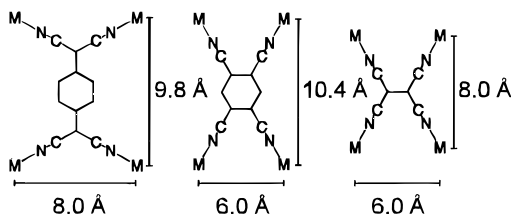


Figure 4. Estimated distances between metal centers in tetranuclear complexes of TCNQ, TCNB, and TCNE (M–N 2.0 Å, C=N 1.1 Å, C–N 1.5 Å, C–C 1.3 Å (TCNE, TCNQ) or 1.4 Å (TCNB)).

The best agreement between experiment and calculation was obtained when axial zero-field splitting was added to the isotropic exchange coupling between the two $S = 1/2$ spins. The Hamiltonian for this model is

$$H = -JS_1S_2 + SDS + \beta SgB \quad (10)$$

Considering an axial symmetry the eigenvalues E values become

$$\begin{aligned} E_1^{\parallel} &= -\frac{J}{4} - \frac{2}{3}D & E_1^{\perp} &= -\frac{J}{4} - \frac{3\beta^2}{D} g_{\perp}^2 B^2 \\ E_2^{\parallel} &= -\frac{J}{4} - \frac{D}{3} - g_{\parallel}\beta B & E_2^{\perp} &= -\frac{J}{4} - \frac{D}{3} \\ E_3^{\parallel} &= -\frac{J}{4} - \frac{D}{3} - g_{\parallel}\beta B & E_3^{\perp} &= -\frac{J}{4} - \frac{D}{3} + \frac{3\beta^2}{D} g_{\perp}^2 B^2 \\ E_4^{\parallel} &= -\frac{3}{4}J & E_4^{\perp} &= -\frac{3}{4}J \end{aligned} \quad (11)$$

Combination of these eigenvalues with the VanVleck equation⁵ yields $\chi_{M^{\parallel}}$ and $\chi_{M^{\perp}}$ which can be averaged to yield χ_M . Neglecting the g anisotropy ($g_{\perp} = g_{\parallel} = g$) one obtains

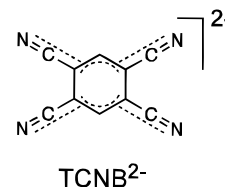
$$\chi_{MT} = \frac{2N\beta^2}{3k} g^2 \left[\frac{e^{-D/3KT}}{e^{2D/3KT} + 2e^{-D/3KT} + e^{-J/KT}} + \frac{\frac{6}{D/kT}(1 - e^{-D/3KT})}{1 + 2e^{-D/3KT} + e^{-J/KT}} \right] + \text{TIP} \times T \quad (12)$$

which was used for curve fitting. The corresponding exchange coupling data are listed in Table 2 and show weak ferromagnetic coupling between the unpaired electrons.

Both the low g factors and the unusually high D values obtained, especially for [Ru₄TCNE], are probably due to the fact that spin–orbit coupling could not be taken into quantitative consideration to account for the magnetic behavior. Attempts to set $J = 0$ resulted in strong disagreement between the simulated and experimental curves. The larger D values for

the ruthenium compounds in comparison to corresponding manganese species reflect the higher spin–orbit coupling constant of Ru ($\approx 1000 \text{ cm}^{-1}$) over Mn ($\approx 250 \text{ cm}^{-1}$).²⁷ Relative to the TCNQ and TCNB analogues, larger J and D values of the complex [Ru₄TCNE] can be attributed to electronic and steric effects permitting stronger coupling across this smallest bridging ligand. Figure 4 illustrates some approximate metal–metal distances in tetranuclear complexes of the TCNX ligands.

The smallest J value found for the TCNQ system correlates with the largest sum of metal–metal distances. Similar correlations can be drawn using the sum of the numbers of intervening bonds, which is largest for TCNQ and smallest for TCNE. Surprisingly, the TCNB ligand fits quite well into such correlations although the free ligand has a distinctly less stabilized π^* acceptor level as compared to TCNE or TCNQ.⁶ This observation strongly supports our successful concept¹⁵ not to consider spin localization on the bridging ligands. However, it is important to note that the first reduction potentials of all three complexes [Ru₄TCNX] are very similar.⁶



Despite the success of model b in the description of the paramagnetism of compounds [Ru₄TCNX], these results only suggest which entities of the complex cations are coupled^{6b} and how they relate to the oxidation state description (eq 4) of the highly symmetric⁶ species. Further studies of these and other such tetranuclear complexes^{10,28} of the TCNX ligands will thus be needed to fully elucidate the electronic structures of these materials, the paramagnetism of organometallic and heavy transition metal 18 valence electron species being of recent interest.²⁹

Acknowledgment. This work was supported by the Franco–German exchange program PROCOPE, and by the Fonds der Chemischen Industrie, Volkswagenstiftung, and Deutsche Forschungsgemeinschaft (Grant SFB 329).

IC960998S

- (27) Felix, F.; Ferguson, J.; Güdel, H. U.; Ludi, A. *J. Am. Chem. Soc.* **1980**, *102*, 4096.
 (28) Baumann, F.; Kaim, W.; Parise, A.; Olabe, J. A.; Jordanov, J. *J. Chem. Soc., Dalton Trans.*, submitted for publication.
 (29) (a) Koeslag, M. A. D.; Hunter, B. K.; MacNeil, J. H.; Roszak, A. W.; Baird, M. C. *Inorg. Chem.* **1996**, *35*, 6937. (b) Smith, M. E.; Andersen, R. A. *J. Am. Chem. Soc.* **1996**, *118*, 11119.